Ukrainian Journal of Physical Optics
ISSUE 3
2024

A NEW SCHEME FOR THE GENERATION OF FREQUENCY 18-TUPLING MM-WAVE SIGNAL BASED ON THREE PARALLEL POLARIZATION MODULATORS

XUEYAO YAN[1], DONGFEI WANG[1,2,*], ZHENZHEN LI[1], XIANGQING WANG[3,4]

[1] School of Information Engineering, Beijing Institute of Graphic Communication, Beijing 102600, China
[2] Nanchang Institute of Technology, Nanchang, Jiangxi Province, 330044, China
[3] School of Physics and Electronic Engineering, Fuyang Normal University, Fuyang, 236037, China
[4] Henan Key Laboratory of Visible Light Communications, Zhengzhou, China
* Corresponding author: wdfchina @126.com

Received: 07.03.2024

Abstract. In work, a new method of optical microwave signal generation with frequency 18-tupling using three parallel polarization modulators (PolMs) was proposed, in which the PolM is integrated through a polarization beam splitter, two phase modulators, an electrical phase shifter, and a polarization beam coupler. To generate a frequency 18-tupling millimeter-wave (mm-wave) signal, the polarization controller must first be employed to bring out linearly polarized light. Next, the linearly polarized light is faded into three PolMs to be modulated by a radio frequency signal, which can achieve multi-frequency optical sidebands. Last, controlling a polarizer to cancel unwanted optical sidebands to obtain ±9th optical sidebands is used to generate an 18-tupling mm-wave signal. We have conducted detailed mathematical formula derivation and computer simulation for the scheme. The results show that the scheme can be experimentally realized and accurate enough with the performance of the signal: the optical sideband suppression ratio can reach 48.02 dB, and the radio frequency spurious suppression ratio can reach 42.25 dB, almost equal to the theoretical model.

Keywords: microwave signal, polarization modulator, optical sideband suppression ratio, radio frequency spurious suppression ratio
UDC: 535.8
DOI: 10.3116/16091833/Ukr.J.Phys.Opt.2024.03019

1. Introduction

Since the 21st century, with the popularity of mobile internet and the continuous growth of people's demand for data transmission, the traffic usage of mobile internet has shown an explosive increase. To meet the flourishing demand for communication and afford more diversified services, we should certainly overcome the existing crowded spectrum and seek a broader range of spectrum resources, especially higher frequency band resources [1-3]. However, the frequency band most services use is mainly concentrated in the small bandwidth of 800 MHz~6 GHz, and the spectrum resources above 10 GHz are rarely utilized [4]. Therefore, if the signal frequency band of the wireless communication system can be expanded to the millimeter wave (mm-wave) band, it can not only solve the problem of spectrum resource shortage but also obtain a faster transmission rate and larger transmission capacity. However, the high path loss and short propagation distance of this high-frequency carrier, the limited spectral response, and the huge cost of current electronic devices also limit the generation of millimeter wave signals by electronic means [5]. Accordingly, optical domain generation of millimeter waves in recent years has received extensive attention from researchers.

There is already some literature available about the photonic generation method of millimeter-wave so far, such as direct modulation techniques [6-8], optical heterodyne methods [9-11], photoelectric oscillators [12-14], and external modulation techniques [15-17]. Among the above methods, the external modulation method is extensively used by most scholars due to its simple structure, high-frequency multiplication factor (FMF), pure signal spectrum, and low-phase noise. Currently, most of the modulators used in external modulation techniques are Mach-Zehnder modulators (MZMs), polarization modulators (PolMs), and the combined dual parallel MZMs (DP-MZM) and the combined dual parallel PolMs (DP-PolM). The existing technology can attain frequency multiplication mm-wave signals with frequency quadrupling, frequency octupling, frequency 12-tupling, frequency 16-tupling, frequency 24-tupling, and so on. For instance, Lin C.T. et al. [18] proposed using two parallel MZMs to obtain an optical mm-wave signal with frequency quadrupling, and the optical sideband suppression ratio (OSSR) is about 36 dB. A frequency-octupled mm-wave signal based on two parallel MZMs with an OSSR of 40 dB is proposed by Zhang Y. et al. [19]. Then Shang L. et al. [20] proposed a frequency octupling method consisting of two cascaded MZMs in parallel, and the OSSR is 40 dB. A scheme proposed by Wang D. et al. [21] to generate a frequency 12-tupling microwave signal using a DP-MZM with an OSSR of about 37.65 dB. Chen X. et al. [22] mentioned that two DP-MZMs cascaded to generate a 16-fold frequency mm-wave signal, and the OSSR is 49 dB. Rani A. et al. in Ref. [23] proposed a scheme of using three cascaded MZMs to generate a frequency 18-tupling mm-wave signal, in which OSSR is 37.98dB and radio frequency spurious suppression ratio (RFSSR) is 32.02 dB. However, the stability of the produced mm-waves is subjected to the bias drift of the MZMs. Consequently, the system based on PolMs to generate mm-wave has been given a rousing reception by researchers because of its two advantages: high extinction ratio and no bias drift. Zhu Z. et al. [24] proposed a photonic generation of frequency-quadrupled and frequency-octupled microwave signals using a DP-PolM. By adjusting the angle of the polarizer, two signals of different frequencies can be obtained using the same set of equipment. The simulated OSSR values were 41.15 dB and 56.36 dB, respectively. The RFSSR values were 35.95 dB and 49.24 dB, individually. Abouelez A.E. et al. [25] proposed two DP-PolMs in parallel to generate a frequency octupling signal with the OSSR at 68.39dB. A frequency 12-tripling signal based on two PolMs in parallel is proposed by Esakki Muthu K. et al. [26], and the OSSR is 37.76 dB. Gayathri S. et al. [27] proposed that a frequency 16-tupling signal is generated using four PolMs in parallel, and the resulting OSSR is 62 dB. Baskaran M. et al. [28] proposed a scheme that uses two cascaded PolMs in parallel, i.e., four modulators used to generate frequency 16-tripling signals, and the OSSR is 63 dB. There are also a few schemes to generate frequency 18-tupling signals. For example, Rani, Ankita, and Deepak Kedia [29] generate an 18-tupled photonic mm-wave using three cascaded MZMs, and the resulting OSSR is 31.5 dB and RFSSR is 32.02 dB. Zhou, Hui, et al. [30] use an external modulator and semiconductor optical amplifier (SOA) to generate an 18-tuple frequency mm-wave; however, when external temperature changes and vibrations occur, which may cause the direct current bias point of the MZM to drift, which requires additional circuits to control and increases the complexity of the system.

To avoid bias point drift and generate higher quality millimeter wave signals, which have high OSSR and RFSSR in the paper, a method of generating highly tunable frequency 18-

tupling mm-wave signal microwave with only three parallel PolMs without an optical filter is proposed. Theoretical analysis and simulation are conducted on the working conditions to achieve the frequency of 18-tupling mm-wave signals. Controlling the phase difference within each PolM, even harmonics can be eliminated, leaving only odd harmonics. Only ninth-order sidebands are attained by suitably adjusting the phase difference among the three PolMs and radio frequency (RF) voltage. The performance of the scheme is discussed in relation to the aspects of OSSR and RFSSR.

2. Principle

This paper proposes a scheme for generating a frequency 18-tupling mm-wave signal based on three PolMs. The PolM contains a polarization beam splitter, two phase shifters, an electrical phase shifter, and a polarization beam coupler, as shown in Fig. 1. Fig. 1 shows a schematic diagram of this system.

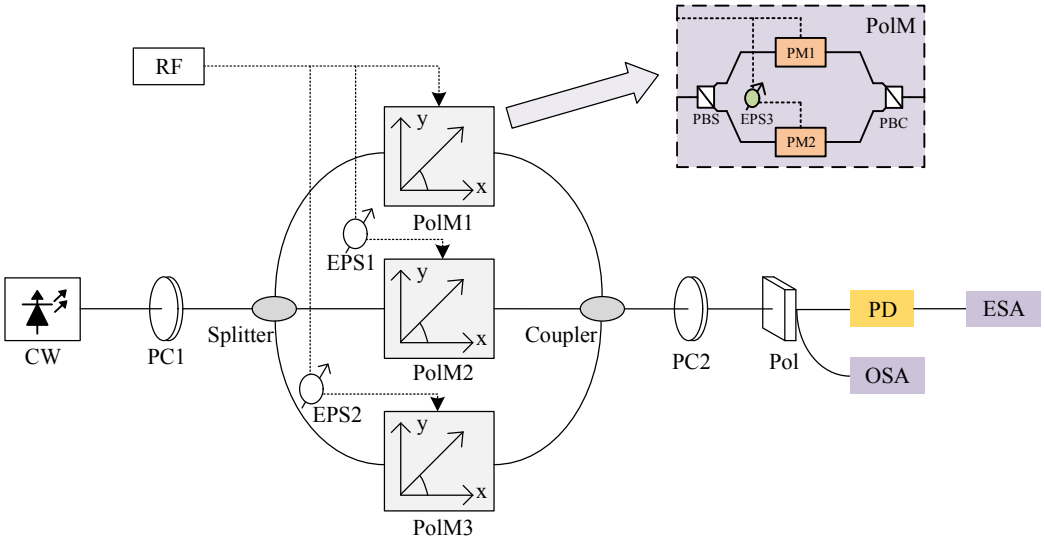

Fig. 1. Schematic diagram of a frequency 18-tupling mm-wave signal generation circuit using three polarization modulators. CW - continuous wave laser; RF - radio frequency; PC1 and PC2 - polarization controllers; EPS1...EPS3 - electrical phase shifters; PolM1...PolM3 - polarization modulators; PBS: polarization beam splitter; PM1 and PM2 - phase modulators; PBC - polarization beam coupler. Pol: polarizer; PD: photodiode; OSA - optical spectrum analyzer; ESA - electrical spectrum analyzer.

A continuous wave (CW) laser emit continuous optical wave signal is defined as $E_{in}(t)=E_c e^{j\omega_c t}$, where E_c and ω_c represent the amplitude and angular frequency of the optical carrier, respectively. The continuous optical wave signal from the CW laser passes through a polarization controller (PC1) by an optical splitter to a polarization modulator (PolM1), and the azimuth of PC1 is θ_1 in respect to the *x*-axis, and then the output signal from PolM1 is:

$$\begin{bmatrix} E_{x1} \\ E_{y1} \end{bmatrix} = E_c e^{j\omega_c t} \begin{bmatrix} \cos\theta_1 e^{jm\sin\omega_m t} \\ \sin\theta_1 e^{-jm\sin\omega_m t - j\varphi_1} \end{bmatrix}, \tag{1}$$

where $m=\pi V_m / V_\pi$ is the modulation index of the polarization modulator (PolM1), V_m is the amplitude of the RF signal, V_π means half-wave voltage, ω_m is the regular frequency of

the RF signal loaded on the PolM, and φ_1 is the phase difference within the PolM1.

Similarly, the output signal from PolM2 and PolM3 can be shown as follows:

$$\begin{bmatrix} E_{x2} \\ E_{y2} \end{bmatrix} = E_c e^{j\omega_c t} \begin{bmatrix} \cos\theta_1 e^{jm\sin(\omega_m t+\varnothing_1)} \\ \sin\theta_1 e^{-jm\sin(\omega_m t+\varnothing_1)-j\varphi_2} \end{bmatrix}, \tag{2}$$

$$\begin{bmatrix} E_{x3} \\ E_{y3} \end{bmatrix} = E_c e^{j\omega_c t} \begin{bmatrix} \cos\theta_1 e^{jm\sin(\omega_m t+\varnothing_2)} \\ \sin\theta_1 e^{-jm\sin(\omega_m t+\varnothing_2)-j\varphi_3} \end{bmatrix}, \tag{3}$$

where $\varnothing_1$ is the phase shift introduced by the first electrical phase shifter (EPS1) and $\varnothing_2$ is the phase shift introduced by the second electrical phase shifter (EPS2), φ_2 and φ_3 is the phase difference within the PolM2 and PolM3, respectively.

Then, the signals output from three polarization modulators are combined at the coupler to form:

$$\begin{aligned} E_{out}(t) &= \frac{1}{3}\begin{bmatrix} E_{x1} \\ E_{y1} \end{bmatrix} + \frac{1}{3}\begin{bmatrix} E_{x2} \\ E_{y2} \end{bmatrix} + \frac{1}{3}\begin{bmatrix} E_{x3} \\ E_{y3} \end{bmatrix} \\ &= \frac{1}{3}E_c e^{j\omega_c t}\left\{ \begin{bmatrix} \cos\theta_1 e^{jm\sin\omega_m t} \\ \sin\theta_1 e^{-jm\sin\omega_m t-j\varphi_1} \end{bmatrix} + \begin{bmatrix} \cos\theta_1 e^{jm\sin(\omega_m t+\varnothing_1)} \\ \sin\theta_1 e^{-jm\sin(\omega_m t+\varnothing_1)-j\varphi_2} \end{bmatrix} + \begin{bmatrix} \cos\theta_1 e^{jm\sin(\omega_m t+\varnothing_2)} \\ \sin\theta_1 e^{-jm\sin(\omega_m t+\varnothing_2)-j\varphi_3} \end{bmatrix} \right\} \\ &= \frac{1}{3}E_c e^{j\omega_c t}\left\{ \begin{bmatrix} \cos\theta_1\left[e^{jm\sin\omega_m t}+e^{jm\sin(\omega_m t+\varnothing_1)}+e^{jm\sin(\omega_m t+\varnothing_2)}\right] \\ \sin\theta_1\left[e^{-jm\sin\omega_m t-j\varphi_1}+e^{-jm\sin(\omega_m t+\varnothing_1)-j\varphi_2}+e^{-jm\sin(\omega_m t+\varnothing_2)-j\varphi_3}\right] \end{bmatrix} \right\}. \end{aligned} \tag{4}$$

The signal from the PC2 is:

$$\begin{aligned} E_{out}(t) &= \frac{1}{3}E_c e^{j\omega_c t} \\ &\times\left\{ \begin{bmatrix} \cos\theta_1\cos\theta_2\left[e^{jm\sin\omega_m t}+e^{jm\sin(\omega_m t+\varnothing_1)}+e^{jm\sin(\omega_m t+\varnothing_2)}\right] \\ \sin\theta_1\sin\theta_2\left[e^{-jm\sin\omega_m t-j\varphi_1}+e^{-jm\sin(\omega_m t+\varnothing_1)-j\varphi_2}+e^{-jm\sin(\omega_m t+\varnothing_2)-j\varphi_3}\right] \end{bmatrix} \right\}, \end{aligned} \tag{5}$$

Where θ_2 is the azimuth of PC2 with respect to the *x*-axis.

Then, the signal from the Pol is:

$$\begin{aligned} E_{out}(t) &= \frac{1}{3}E_c e^{j\omega_c t} \\ &\times\begin{bmatrix} \cos\theta_3 & 0 \\ 0 & \sin\theta_3 \end{bmatrix} \\ &\times\left\{ \begin{bmatrix} \cos\theta_1\cos\theta_2\left[e^{jm\sin\omega_m t}+e^{jm\sin(\omega_m t+\varnothing_1)}+e^{jm\sin(\omega_m t+\varnothing_2)}\right] \\ \sin\theta_1\sin\theta_2\left[e^{-jm\sin\omega_m t-j\varphi_1}+e^{-jm\sin(\omega_m t+\varnothing_1)-j\varphi_2}+e^{-jm\sin(\omega_m t+\varnothing_2)-j\varphi_3}\right] \end{bmatrix} \right\}, \end{aligned} \tag{6}$$

Here θ_3 is the polarization angle of Pol.

To suppress even-order optical sidebands, we can set the azimuth of PC1 θ_1 to $\pi/4$, the azimuth of PC2 θ_2 to $\pi/2$, and the polarization angle of Pol θ_3 to $\pi/4$, then the output optical signal can be defined as:

$$E_{out}(t)=\frac{1}{6}E_c e^{j\omega_c t}\left[e^{jm\sin\omega_m t}+e^{-jm\sin\omega_m t-j\varphi_1}\right]$$
$$+\frac{1}{6}E_c e^{j\omega_c t}\left[e^{jm\sin(\omega_m t+\varnothing_2)}+e^{-jm\sin(\omega_m t+\varnothing_2)-j\varphi_2}\right]. \quad (7)$$
$$+\frac{1}{6}E_c e^{j\omega_c t}\left[e^{jm\sin(\omega_m t+\varnothing_3)}+e^{-jm\sin(\omega_m t+\varnothing_3)-j\varphi_3}\right]$$

Using the Bessel function to expand Eq. (7), we can get:

$$E_{out}(t)=\frac{1}{6}E_c e^{j\omega_c t}$$
$$\times\sum_{n=-\infty}^{\infty}\left\{J_n(m)e^{jn\omega_m t}\begin{bmatrix}1+(-1)^n e^{-j\varphi_1}+e^{jn\varnothing_2}+(-1)^n e^{jn\varnothing_2}e^{-j\varphi_2}\\+e^{jn\varnothing_3}+(-1)^n e^{jn\varnothing_3}e^{-j\varphi_3}\end{bmatrix}\right\}, \quad (8)$$

where $J_n(m)$ is the Bessel function of the first kind of *n*-th order, and *m* is the modulation index.

When the phase difference of the PolM $\varphi_1=\varphi_2=\varphi_3=\pi$, Eq. (8) can be simplified as:

$$E_{out}(t)=\frac{1}{6}E_c e^{j\omega_c t}$$
$$\times\sum_{n=-\infty}^{\infty}\left\{J_n(m)e^{jn\omega_m t}\left[1-(-1)^n\right]\left[1+e^{jn\varnothing_2}+e^{jn\varnothing_3}\right]\right\}, (n=1,3,5,7,9,\ldots), \quad (9)$$

Due to the $\left[1-(-1)^n\right]$ term in Eq. (9), when the value of *n* is even (0, 2, 4, 6 ...), all even-order sidebands would be suppressed, then Eq. (9) can be written as:

$$E_{out}(t)=\frac{1}{3}E_c e^{j\omega_c t}$$
$$\times\begin{Bmatrix}J_1(m)e^{j\omega_m t}\left[1+e^{j\varnothing_2}+e^{j\varnothing_3}\right]\\+J_3(m)e^{j3\omega_m t}\left[1+e^{j3\varnothing_2}+e^{j3\varnothing_3}\right]\\+J_5(m)e^{j5\omega_m t}\left[1+e^{j5\varnothing_2}+e^{j5\varnothing_3}\right]\\+J_7(m)e^{j7\omega_m t}\left[1+e^{j7\varnothing_2}+e^{j7\varnothing_3}\right]\\+J_9(m)e^{j9\omega_m t}\left[1+e^{j9\varnothing_2}+e^{j9\varnothing_3}\right]+\ldots\end{Bmatrix} \quad (10)$$

It can be seen from Eq. (10) to suppress the unwanted third-order optical sidebands, we can adjust the modulation index *m*=6.380, which can be seen in Fig. 2. Besides, to contain the unwanted first, fifth and seventh-order optical sidebands, the phase difference of the first electrical phase shifter (EPS1) with $\varnothing_1$ is set to $2\pi/3$, and the phase difference of the second electrical phase shifter (EPS2) with $\varnothing_2$ is configured to $-2\pi/3$, so that $1+e^{(\pm jn\varnothing_2)}+e^{(\pm jn\varnothing_3)}=0,\ n=1,5,7$ is satisfied.

Then Eq. (10) can be written as:

$$E_{out}(t)=\frac{1}{3}E_c e^{j\omega_c t}$$
$$\times\left\{J_9(m)e^{j9\omega_m t}\left[1+e^{j9\varnothing_2}+e^{j9\varnothing_3}\right]+\ldots\right\}. \quad (11)$$

Meanwhile, there are only two ninth-order sidebands at the optical coupler's output, so we can acquire an mm-wave signal of frequency 18-tupling mm-wave signal with two ninth-order sidebands.

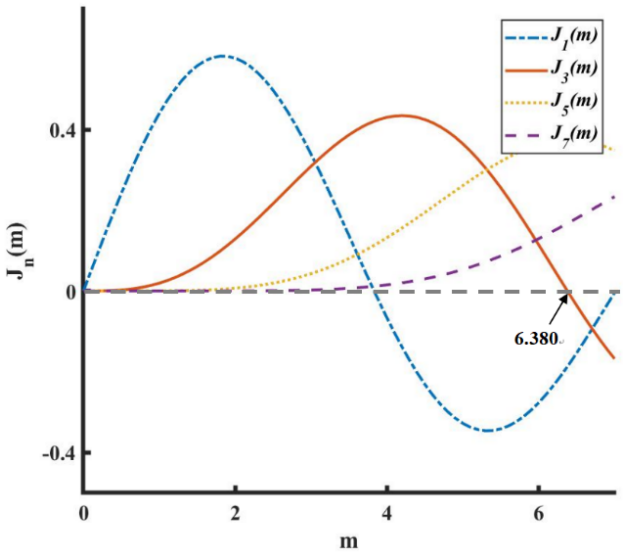

Fig. 2. Graph of the Bessel function of the first kind of first, third, fifth, and seventh order.

When m=6.380, due to some unsatisfactory factors, the third-order optical sidebands are not completely eliminated, becoming the optical sidebands with the highest amplitude except for the ninth-order optical sidebands, so according to the definition of OSSR, it can be obtained that:

$$OSSR \approx 10\log_{10}\left[\frac{J_9^2(6.380)}{J_3^2(6.380)}\right] = 48.02\,\text{dB}\,. \tag{12}$$

These sidebands are then allowed to beat at the PD, and the resulting photocurrent can be expressed as:

$$\begin{aligned} I(t) &\propto \Re \mathrm{E}_c^2\left[J_3(m)\cos 3\omega_m t + J_9(m)\cos 9\omega_m t\right]^2 \\ &= \Re \mathrm{E}_c^2\begin{bmatrix} J_3^2(m)\cos^2 3\omega_m t + J_9^2(m)\cos^2 9\omega_m t \\ +2J_3(m)J_9(m)\cos 3\omega_m t\,\cos 9\omega_m t \end{bmatrix} \\ &= \Re \mathrm{E}_c^2\begin{bmatrix} J_3^2(m)\left(\dfrac{1+\cos 6\omega_m t}{2}\right) + J_9^2(m)\left(\dfrac{1+\cos 18\omega_m t}{2}\right) \\ +J_3(m)J_9(m)\left(\cos 6\omega_m t + \cos 12\omega_m t\right) \end{bmatrix}, \end{aligned} \tag{13}$$

where $\Re$ is the responsivity of the PD.

Similarly, it can be concluded according to the definition of RFSSR

$$RFSSR \approx 10\log_{10}\left[\frac{J_9^2(6.380)}{J_3^2(6.380)}\right] = 42.25\,\text{dB}\,. \tag{14}$$

3. Simulation results and analysis

A simulation experiment software is used for simulation and confirmation to verify the accuracy of the generated frequency 18-tupling mm-wave signals. Table 1 shows the parameter settings of the main components in the simulation.

A continuous laser with a linewidth of 10 MHz and a frequency of 193.1 THz is uniformly divided into three beams by a splitter and injected into three parallel PolMs, driven by an RF at 10GHz. The modulation index of the three modulators is set to 6.380, the

phase difference of the EPS1 with $\varnothing_1$ is set to $2\pi/3$, and the phase difference of EPS2 with $\varnothing_2$ is configured to $-2\pi/3$.

Table 1. The main component parameters involved in the simulation.

Parameters	Values
The center frequency of CW laser	193.1 THz
Linewidth of CW laser	10 MHz
Power of CW laser	20 dBm
Frequency of RF	10 GHz
Azimuth of PC1	$\pi/4$
Azimuth of PC2	$\pi/2$
The phase shift of EPS1	$2\pi/3$
The phase shift of EPS2	$-2\pi/3$
Polarization angle of Pol	$\pi/4$
Responsivity of PD	0.8 A/W
The dark current of PD	10 nA

It is demonstrated that this plan using three parallel PolMs to generate a frequency 18-tupling mm-wave signal is logical by observing the simulation results. A higher multiplication factor is achieved without an optical filter, resulting in an OSSR of 48.02 dB and an RFSSR of 42.25 dB. Owing to the frequency-tuneable type of the scheme, a signal of 180 GHz can be produced. The output optical spectrum diagram is shown in Fig. 3, and (a) in Fig. 3 displays the simulation output optical spectrum of the output signal behind the coupler. The final signal detected by the optical spectrum analyzer (OSA) is shown in Fig. 3(b). The ±9th-order sidebands are the main sidebands, located at 193.01 THz and 193.19 THz separately, with an interval of 180 GHz, 18 times the frequency of the 10 GHz RF driving signal.

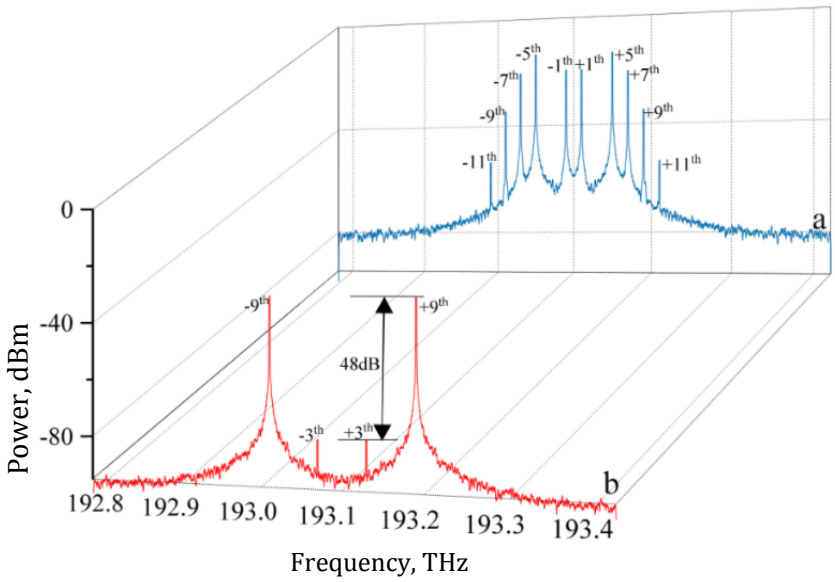

Fig. 3. The simulated output optical spectrum detected by optical spectrum analyzer: (a) without adjusting of modulation index and phase shifts; (b) with adjusting of modulation index and phase shifts.

Fig. 4 shows the simulation output RF spectrum by photodiode (PD). The maximum RF signal power is generated at 180 GHz, which is the required 18th RF signal.

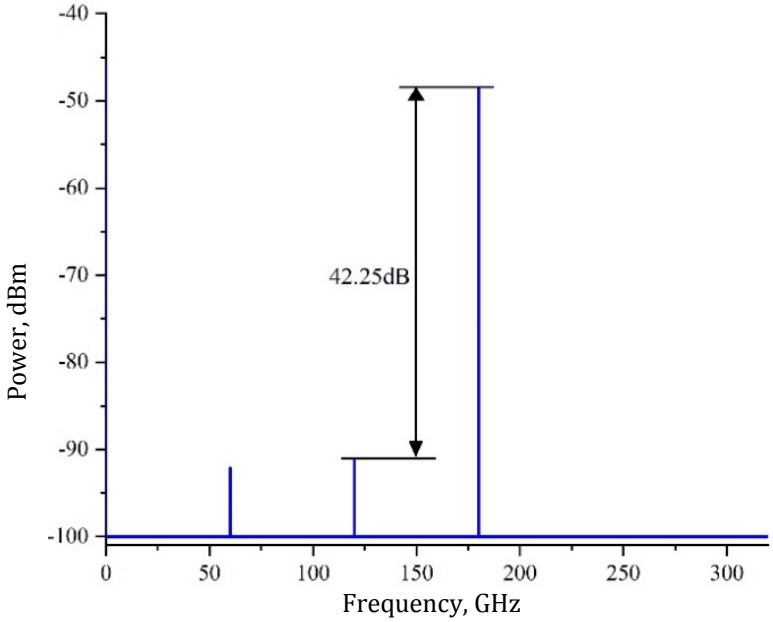

Fig. 4. Output diagram of RF spectrum.

As presented above, by adjusting the azimuth of the PC1 and PC2, the polarization angle of Pol, and the phase difference of the EPS1 and EPS2, the high-purity 18-tupling frequency signal can be gained. The simulation results prove that this proposed scheme can generate microwave signals with high-frequency multiplication factors without an optical filter and only using three polarization modulators, achieving a large variable range of frequencies. However, these parameters may depart from the mathematical calculation value. Thus, it is vital to investigate the impact of these non-ideal elements on OSSR and RFSSR.

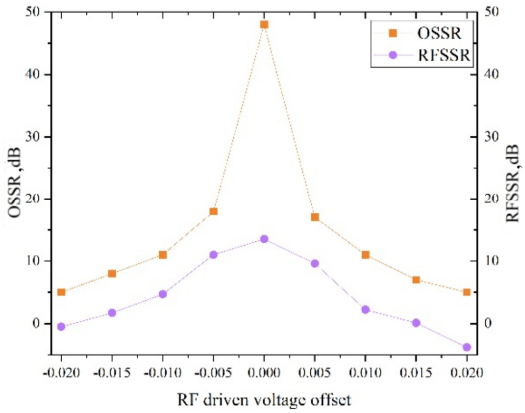

Fig. 5 The impact of RF-driven voltage on OSSR and RFSSR.

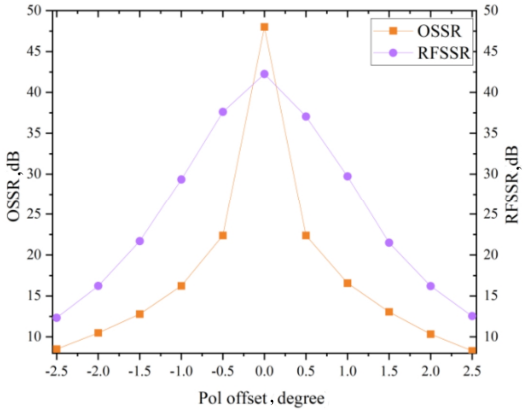

Fig. 6 The influence of Pol angle drift on OSSR and RFSSR.

The impact of non-ideal RF-driven voltage on OSSR and RFSSR for frequency 18-tupling mm-wave signal is shown in Fig. 5. It can be seen that a deviation of only ±0.001 in RF input voltage will have a significant influence on OSSR and RFSSR. When the RF voltage approaches the calculated value, the OSSR and RFSSR of the signal gained are the highest and will decrease

as the deviation increases. The outcome obtained is still admissible if the deviation is less than ±0.005. The OSSR value is over 15 dB. But if the deviation exceeds ±0.002, the calculated RFSSR value is no longer ideal.

Since the scheme of this simulation uses a polarizer before signal output, the influence of polarizer angle drift on OSSR and RFSSR is shown in Fig. 6. The function of the Pol is to work with PC1 to achieve the peak of the PolMs when $\theta_1 = \pi/4$, $\theta_2 = \pi/4$ are mentioned in principle section, which is to suppress even order optical sidebands. We can see that when the error does not exceed ±1 deg, the OSSR value is above 15 dB; when the error does not exceed ±2 deg, the RFSSR value is above 15 dB. Therefore, the deviation of the polarizer angle should not exceed ±2 deg as much as possible.

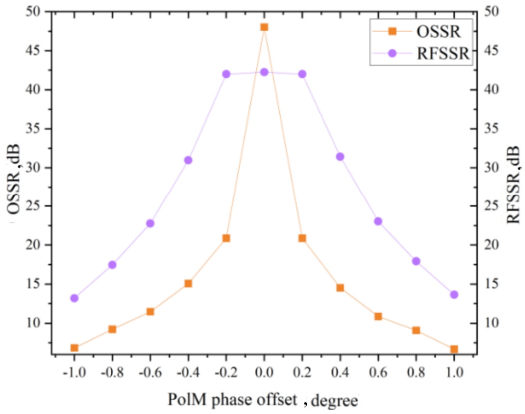

Fig. 7. The effect of phase difference within PolM on OSSR and RFSSR.

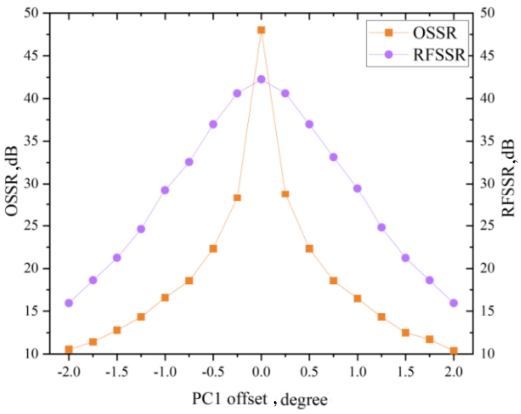

Fig. 8. The impact of PC1 angle drift on OSSR and RFSSR.

Fig. 7 shows the effect of phase difference within a PolM on OSSR and RFSSR. It can be seen that when the deviation is less than ±0.2 deg, the obtained RFSSR is not significantly different from the theoretical value. So, an error within ±0.8 deg is acceptable for RFSSR. For OSSR, once there is a small change, other orders of signal will exist, which will affect the purity of the signal.

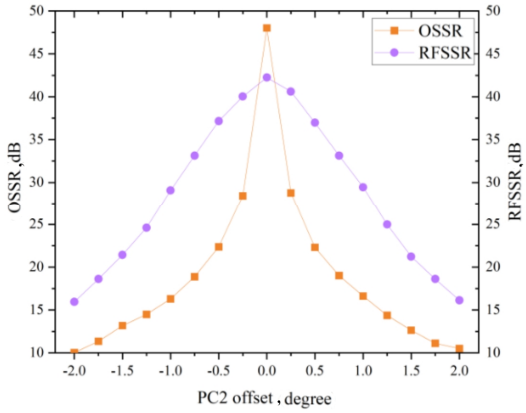

Fig. 9. The effect of PC2 angle drift on OSSR and RFSSR.

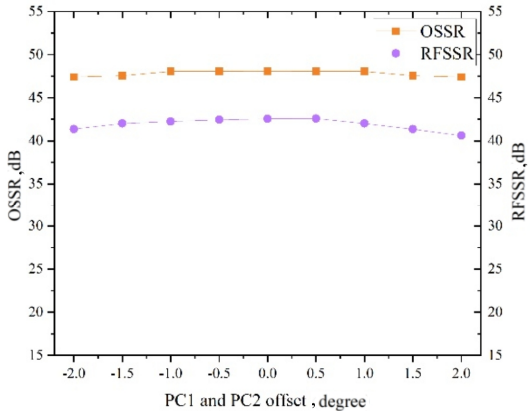

Fig. 10. The impact of simultaneous offset of PC1 and PC2 on OSSR and RFSSR.

There are also two polarization controllers to adjust the working mode of three polarization modulators in this scheme, so the angular deviation of the two polarization controllers can also lead to errors in the simulation results. Then, the impact of PC1's angular

deviation on OSSR and RFSSR is shown in Fig. 8. It can be seen from the figure that when PC1 deviates by ±0.25 deg, the value of OSSR decreases significantly but remains above 15 dB when the drift is not exceeded ±1 deg. As the deviation angle increases, the OSSR value gradually decreases until the deviation exceeds ±2 deg and the value approaches 10dB. At this point, the ±6th-order sidebands will beat to produce 12-tupling frequency signal.

The influence of the angle deviation of PC2 on OSSR and RFSSR is shown in Fig. 9. Similar to the analysis in Fig. 8, the error is allowed within ±1 degree, and the OSSR of mm-wave signals is above 15 dB. But when the deviation exceeds 2 deg, the error cannot be ignored. Then, we can see that if the azimuth of polarization is changed in both PC1 and PC2, the values of OSSR and RFSSR do not deviate greatly, as shown in Fig. 10.

4. Conclusion

A method to achieve an mm-wave signal of frequency 18-tupling mm-wave signal using three PolMs is proposed. Through reasonably controlling the polarization direction of the PC after the parallel PolMs, the polarization angle of the polarizer and the voltage and phase of the RF driven voltage, a frequency 18-tupling mm-wave signal microwave signal with an OSSR of 48.02 dB and an RFSSR of 42.25 dB can be generated. Moreover, the effects of several non-ideal factors on OSSR and RFSSR have also been researched. The simulation results demonstrate that even if those affected elements, such as RF voltage, angle drift of Pol, phase difference within PolM, and angle drift of PC, as long as they deviate within a certain extent from the ideal value, the consequence is still admissible. Compared with the previous schemes using PolMs, this scheme only uses three polarization modulators in parallel, and the 18-tupling signal is acquired without the filter condition; the obtained signal is pure, and the system is steady.

Declaration of competing interest. The authors declare no conflicts of interest.

Acknowledgements. This work was supported by the R&D Program of Beijing Municipal Education Commission (KM202310015002), the Open Project of Tianjin Key Laboratory of Optoelectronic Detection Technology and System (2023LOTDS019), the Open Project Program of Shanxi Key Laboratory of Advanced Semiconductor Optoelectronic Devices and Integrated Systems (2023SZKF21) and Jiangxi Provincial Natural Science Foundation (20232BAB212006). This research work was supported in part by the Scientific Research Project of Fuyang Normal University (2022KYQD0004) and Anhui Education Department, and the University Natural Science Research Project of Anhui Province (2022AH051338). This work Municip is supported by Henan Key Laboratory of Visible Light Communications (HKLVLC2023-B10). The Youth Excellent Project of Beijing Institute of Graphic Communication(Ea202411).

References

1. Wang, D., Zhang, Y., Yang, Z., Zhang, L., Wu, B., Yang, X., Yan,S. & Wang, X. (2024). A new filterless W-band millimeter wave signals generation scheme with frequency octupling based on cascaded Mach-Zehnder modulators.. *Ukrainian Journal of Physical Optics*, *25*(1).
2. Wang, D., Li, Y., Yan, X., Ding, H., & Li, Z. (2023). A simple filter-less QPSK modulated vector millimeter-wave signal generation with frequency quadrupling only enabled by a DP-PolM. *Optical and Quantum Electronics*, *55*(14), 1244.
3. Zeb, K., Lu, Z. G., Liu, J. R., Rahim, M., Pakulski, G., Poole, P. J., Mao, Y.X., Song, C.Y. Barrios, P. Jiang, W.H. & Zhang, X. (2019, October). Photonic generation of spectrally pure millimeter-wave signals for 5G applications. In *2019 International Topical Meeting on Microwave Photonics (MWP)* (pp. 1-4). IEEE.

4. Gomes, N. J., Monteiro, P. P., & Gameiro, A. (2012). *Next generation wireless communications using radio over fiber*. John Wiley & Sons.
5. Li, X., Yu, J., Zhang, J., Xiao, J., Zhang, Z., Xu, Y., & Chen, L. (2015). QAM vector signal generation by optical carrier suppression and precoding techniques. *IEEE Photonics Technology Letters*, *27*(18), 1977-1980.
6. Davies, P. A., Foord, A. P., & Razavi, K. E. (1995). Millimeter-wave signal generation by optical filtering of frequency-modulated laser spectra. *Electronics Letters*, *31*(20), 1754-1756.
7. Ray, S., Médard, M., & Zheng, L. (2011). Fiber aided wireless network architecture. *IEEE Journal on selected areas in Communications*, *29*(6), 1284-1294.
8. Rivera-Silva, V., Millan-Mejia, A. J., & Gutiérrez-Castrejón, R. (2012, September). Automatic classification of the frequency chirp in directly modulated lasers using cross-correlation. In *2012 9th International Conference on Electrical Engineering, Computing Science and Automatic Control (CCE)* (pp. 1-6). IEEE.
9. Wen, Y. J., Liu, H. F., Novak, D., & Ogawa, Y. (2000). Millimeter-wave signal generation from a monolithic semiconductor laser via subharmonic optical injection. *IEEE Photonics Technology Letters*, *12*(8), 1058-1060.
10. Li, J., Ning, T., Pei, L., Qi, C., Zhou, Q., Hu, X., & Gao, S. (2010). 60 GHz millimeter-wave generator based on a frequency-quadrupling feed-forward modulation technique. *Optics Letters*, *35*(21), 3619-3621.
11. Feng, X., Yang, P., He, L., Niu, F., Zhong, B., & Xu, H. (2016). Heterodyne system for measuring frequency response of photodetectors in ultrasonic applications. *IEEE Photonics Technology Letters*, *28*(12), 1360-1362.
12. Jin, S., Duan, R., Xiao, L., Zhu, H., Li, D., & Wang, T. (2021, October). Based on Brillouin Scattering Photoelectric Research of Oscillator. In *2021 13th International Conference on Advanced Infocomm Technology (ICAIT)* (pp. 16-19). IEEE.
13. Zhang, K., Li, S., Xie, Z., & Zheng, Z. (2022). An all-optical Ka-band microwave long-distance dissemination system based on an optoelectronic oscillator. *IEEE Photonics Journal*, *14*(4), 1-5.
14. Liu, H., Yang, J., Sun, T., & Wang, J. (2022, December). Coupled optoelectronic oscillator and its application in 5G communication system. In *Fifth International Conference on Mechatronics and Computer Technology Engineering (MCTE 2022)* (Vol. 12500, pp. 125-130). SPIE.
15. Wang, D., Wang, X., Yang, X., Gao, F., Zhang, L., Yang, Z., & Wu, B. (2023). Photonic filter-free adjustable frequency sextupling scheme for V-band vector mm-wave signal generation based on a DP-MZM with precoding. *Optics Communications*, *545*, 129633.
16. Prem, A., & Chakrapani, A. (2017). Optical millimeter wave generation using external modulation--a review. *Advances in Natural and Applied Sciences*, *11*(1), 8-13.
17. Dar, A. B., & Ahmad, F. (2022). Optical millimeter-wave generation techniques: An overview. *Optik*, *258*, 168858.
18. Lin, C. T., Shih, P. T., Chen, J., Xue, W. Q., Peng, P. C., & Chi, S. (2008). Optical millimeter-wave signal generation using frequency quadrupling technique and no optical filtering. *IEEE Photonics Technology Letters*, *20*(12), 1027-1029.
19. Zhang, Y., & Pan, S. (2012, September). Experimental demonstration of frequency-octupled millimeter-wave signal generation based on a dual-parallel Mach-Zehnder modulator. In *2012 IEEE MTT-S International Microwave Workshop Series on Millimeter Wave Wireless Technology and Applications* (pp. 1-4). IEEE.
20. Shang, L., Wen, A., Li, B., Wang, T., & Chen, Y. (2012). A filterless optical millimeter-wave generation based on frequency octupling. *Optik*, *123*(13), 1183-1186.
21. Wang, D., Tang, X., Fan, Y., Zhang, X., Xi, L., & Zhang, W. (2018, November). A new approach to generate the optical millimeter-wave signals using frequency 12-tupling without an optical filter. In *Tenth International Conference on Information Optics and Photonics* (Vol. 10964, pp. 280-284). SPIE.
22. Chen, X., Liu, Z., Jiang, C., & Huang, D. (2013, November). A filterless optical millimeter-wave generation based on frequency 16-tupling. In *Asia Communications and Photonics Conference* (pp. AF3B-4). Optica Publishing Group.
23. Rani, A., & Kedia, D. (2023). An 18-tupled photonic millimeter-wave generation using cascaded Mach-Zehnder modulators. *Fiber and Integrated Optics*, *42*(1), 1-19.
24. Zhu, Z., Zhao, S., Li, X., Huang, A. Q., Qu, K., & Lin, T. (2016). Photonic generation of frequency-octupled and frequency-quadrupled microwave signals using a dual-parallel polarization modulator. *Optical and Quantum Electronics*, *48*, 1-12.
25. Abouelez, A. E. (2020). Optical millimeter-wave generation via frequency octupling circuit based on two parallel dual-parallel polarization modulators. *Optical and Quantum Electronics*, *52*(10), 439.
26. Esakki Muthu, K., & Sivanantha Raja, A. (2018). Millimeter wave generation through frequency 12-tupling using DP-polarization modulators. *Optical and Quantum Electronics*, *50*(5), 227.

27. Gayathri, S., & Baskaran, M. (2019, March). Frequency 16 tupling technique with the use of four parallel polarization modulators. In *2019 International Conference on Wireless Communications Signal Processing and Networking (WiSPNET)* (pp. 282-286). IEEE.
28. Baskaran, M., Prabakaran, R., & Gayathri, T. S. (2019). Photonic generation of frequency 16-tupling millimeter wave signal using polarization property without an optical filter. *Optik*, *184*, 348-355.
29. Rani, A., & Kedia, D. (2023). An 18-tupled photonic millimeter-wave generation using cascaded Mach-Zehnder modulators. *Fiber and Integrated Optics*, *42*(1), 1-19.
30. Zhou, H., Fei, C., Zeng, Y., Tan, Y., & Chen, M. (2021). A ROF system based on 18-tuple frequency millimeter wave generation using external modulator and SOA. *Optical Fiber Technology*, *61*, 102402.

Xueyao Yan, Dongfei Wang, Zhenzhen Li, Xiangqing Wang. (2024). A new scheme for the generation of frequency 18-tupling mm-wave signal based on three parallel polarization modulators. *Ukrainian Journal of Physical Optics*, *25*(3), 03019 – 03030.
doi: 10.3116/16091833/Ukr.J.Phys.Opt.2024.03019

Анотація. *У роботі запропоновано новий метод генерації оптичного мікрохвильового сигналу з 18-кратною частотою з використанням трьох паралельних поляризаційних модуляторів (PolM), в якому PolM об'єднаний через поляризаційний розгалужувач променя, два фазові модулятори, електричний фазозсувач і поляризаційний об'єднувач променя. Для генерації сигналу міліметрового діапазону з 18-ти кратним помноженням необхідно задіяти контролер поляризації. Далі лінійно поляризоване світло перетворюється на три промені, які модулюються PolM радіочастотним сигналом, що дозволяє отримати багаточастотні оптичні бічні смуги. Нарешті, керування поляризатором для усунення небажаних оптичних бічних смуг для отримання ±9 оптичних бічних смуг використовується для генерації 18-кратного сигналу мм-хвиль. Нами отримані математичні співвідношення та здійснене комп'ютерне моделювання цієї схеми. Результати показують, що схема може бути експериментально реалізованою з досить точними характеристиками сигналу: коефіцієнт придушення оптичної бічної смуги може досягати 48,02 дБ, а коефіцієнт придушення паразитних частот може досягати 42,25 дБ, що відповідає теоретичній моделі.*

Ключові слова: *мікрохвильовий сигнал, поляризаційний модулятор, коефіцієнт придушення оптичної бічної смуги, коефіцієнт придушення паразитних частот*